Sudden Change Events of Plasma Current during Electron-Cyclotron Current Start-Up on the QUEST Spherical Tokamak*)

Ryuya IKEZOE, Kosuke TAKEDA[1)], Kengoh KURODA[a)], Takumi ONCHI, Takahiro NAGATA, Izumi SEKIYA, Hiroshi IDEI, Fadilla ZENNIFA, Yifan ZHANG[1)], Seiya SAKAI[1)], Rikuya MIYATA[1)], Takahiro YAMAGUCHI[1)], Makoto HASEGAWA, Yoshihiko NAGASHIMA, Takeshi IDO and Kazuaki HANADA

Research Institute for Applied Mechanics, Kyushu University, Fukuoka 816-8580, Japan
[1)]*Interdisciplinary Graduate School of Engineering Sciences, Kyushu University, Fukuoka 816-8580, Japan*

(Received 9 January 2023 / Accepted 27 June 2023)

Non-inductive plasma current start-up experiments have been conducted using 2nd harmonic electron-cyclotron resonance heating (ECRH) on the QUEST spherical tokamak. Sudden or abrupt changes in plasma current, referred to as sudden change events (SCEs), have been frequently observed during these experiments. To investigate these events, fast magnetic activity was measured globally by installing arrays of magnetic pick-up coils inside the vacuum vessel on QUEST. Analysis revealed that all observed SCEs could be classified into three categories based on their magnetic characteristics. In one type of event, called SCE–III, the plasma current suddenly decreases by up to 50% instantaneously, occurring in a wide discharge region achieved using 2nd ECRH start-up on QUEST. These SCE–III events may potentially lead to disruptions in future discharges at higher powers.

Keywords: spherical tokamak, non-inductive current start-up, abrupt phenomena, MHD, magnetic fluctuation, IRE

DOI: 10.1585/pfr.18.2402066

1. Introduction

Non-inductive plasma current start-up has been investigated using 2nd harmonic electron-cyclotron heating and current drive on the QUEST spherical tokamak (ST) [1–3]. Prior research indicates that current drive efficiency can vary by tens to hundreds of times depending on the generation of energetic electrons. Recently, the EXL-50 experiment (ST in China) also demonstrated the advantageous properties of energetic electrons as efficient conducting carriers [4]. The production of energetic electrons can be significantly enhanced due to their exceptional absorption efficiency, which results from relativistic Doppler broadening and infrequent collisions with bulk plasma at higher energies. Oblique injection of the 2nd X-mode in QUEST effectively accelerates energetic electrons rotating in one direction, as the majority of power is absorbed at the upshift resonance while the down-shift resonance region is blocked by the center stack on QUEST [5].

To devise an electron-cyclotron (EC) plasma current start-up scenario based on the QUEST results, it is crucial to identify a control method that prevents runaway electron issues and to examine the effects of energetic electrons on properties such as general magnetohydrodynamic (MHD) behavior [6]. This paper focuses on the latter research topic.

A distinctive phenomenon observed during EC start-up discharges on QUEST is the rapid decay of plasma current. These events manifest suddenly, accompanied by bright visible emissions when monitored using a high-speed camera. The sudden and irregular reductions in plasma current pose a challenge to achieving a smooth current ramp-up. Motivated by the sudden change events (SCEs) in plasma current, this study investigates magnetic fluctuations associated with SCEs by installing magnetic pick-up coils throughout the QUEST vacuum vessel. This paper presents and categorizes all observed sudden phenomena in QUEST using new measurement results.

The remainder of this paper is organized as follows: Section 2 introduces the newly implemented magnetic sensors, while Section 3 presents a comprehensive account of all sudden events observed thus far in QUEST. Sections 4 and 5 provide discussion and a summary of this study, respectively.

2. Magnetic Pick-Up Coils

Since the typical time constant of the observed phenomena is much faster than the field penetration time of

author's e-mail: ikezoe@triam.kyushu-u.ac.jp
[a)]*Present address: Japan Coast Guard Academy, Kure, Hiroshima, Japan*
*) This article is based on the presentation at the 31st International Toki Conference on Plasma and Fusion Research (ITC31).

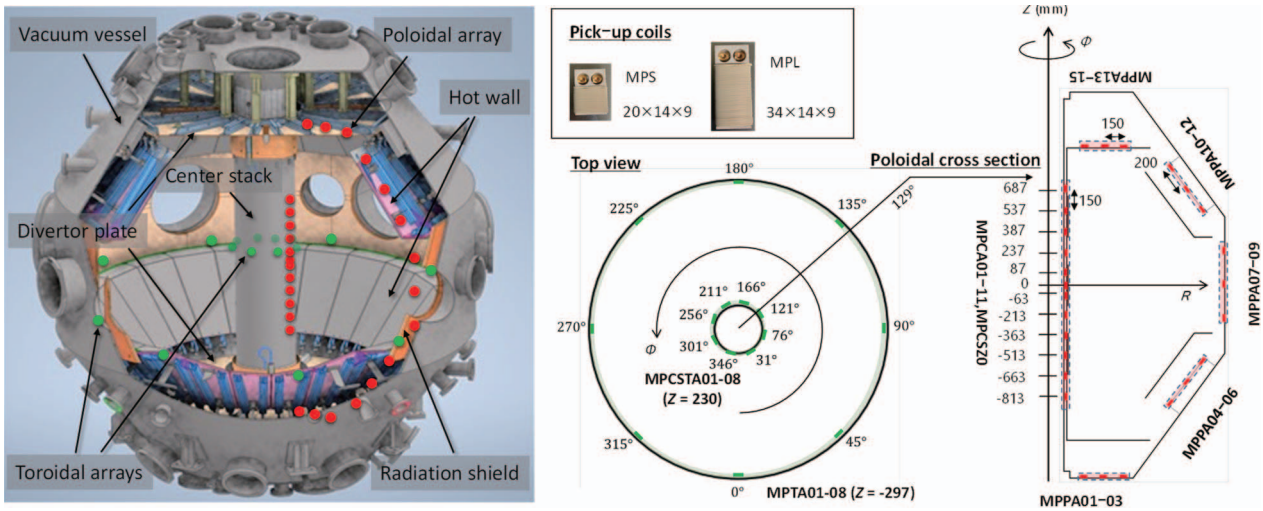

Fig. 1 Schematic view of QUEST vacuum vessel components and arrangement of magnetic pick-up coils.

the vacuum vessel, all the coils were designed for fast response and installed inside the vacuum vessel to meet various conditions.

QUEST conducts long-pulse plasma discharges under the control of particle recycling using a hot wall, which can reach temperatures of up to 500°C. Due to the large number of coils required, polyetheretherketone (PEEK) was used as the insulating material for both the bobbin and wire, instead of more expensive ceramics. PEEK's heat resistance is nominally 250°C. All the coils were installed in locations with relatively lower temperatures, even when the hot wall was heated; the vacuum vessel itself is maintained below 150°C in order to protect the vacuum vessel from breaking due to thermal expansion. The arrangement of the coils and the vacuum vessel components of QUEST is illustrated in Fig. 1. As can be seen from the figure, a toroidal array, consisting of 8 coils, and the inner part of a poloidal array are mounted behind the segmented panels surrounding the center stack. These coils measure $20 \times 14 \times 9$ in size and have an effective cross-sectional area of approximately 50 cm^2, detecting the Z component of the magnetic field. Another toroidal array and the outer part of the poloidal array are situated on the vessel wall behind three-layer radiation shields. Due to the presence of a 1 mm thick copper panel as the third layer of the radiation shield, the frequency response was, unfortunately, expected to be significantly lower. Hot walls are situated in both the top and bottom conical regions, with each consisting of 20 toroidally arranged hot panels. One of these panels is a dummy panel, connected to adjacent panels for heat conduction, behind which the outer part of the poloidal array is installed. Additionally, three coils are installed behind both the top and bottom divertor plates, using a base created by folding a thin stainless steel (SS) plate to inhibit heat conduction from the divertor plates.

The coils installed in locations other than the center stack detect poloidal field components with an effective cross-sectional area approximately 100 cm^2. The frequency response is depicted in Fig. 2, showing a linear frequency response for amplitude and phase confirmed to be well over 500 kHz.

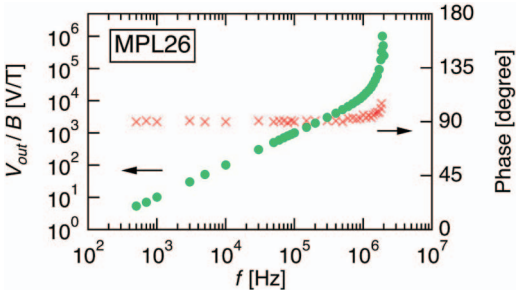

Fig. 2 Frequency response of pick-up coil of approximately 100 cm^2 effective cross section. Circle and cross plots show output voltage normalized with applied magnetic field strength and output phase shifting, respectively.

All coil signals are transmitted using twisted cables to a multi-channel insulated amplifier with a 1 MHz bandwidth, featuring selectable attenuators, low-pass filters, and amplifiers (custom-order, Tsuji Denshi Co., Ltd.). The signals are then digitized at a sampling rate of either 200 kHz or 1 MHz. As this work focuses on fast phenomena, all measurements were sampled using the same digitizer to eliminate any time lag.

3. Experimental Results

3.1 SCE–I: repeated decays during current ramp-up

In 2nd electron-cyclotron (EC) start-up discharges using a 28 GHz Gyrotron on QUEST, repetitive current decay events sometimes occur. For convenience, these events are referred to as SCE–I in this paper. Typical waveforms of plasma current (I_p) are shown alongside line-integrated

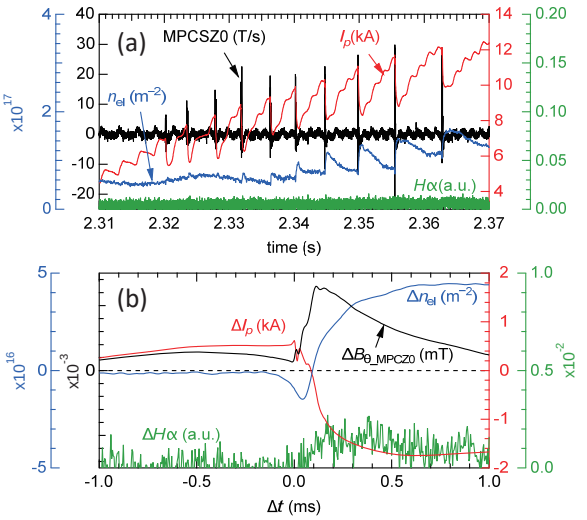

Fig. 3 Spikes in magnetic field at sudden plasma current decays along with a line integrated density and an H_α emission intensity. (b) is expanded waveforms that are conditionally ensemble-averaged for large events.

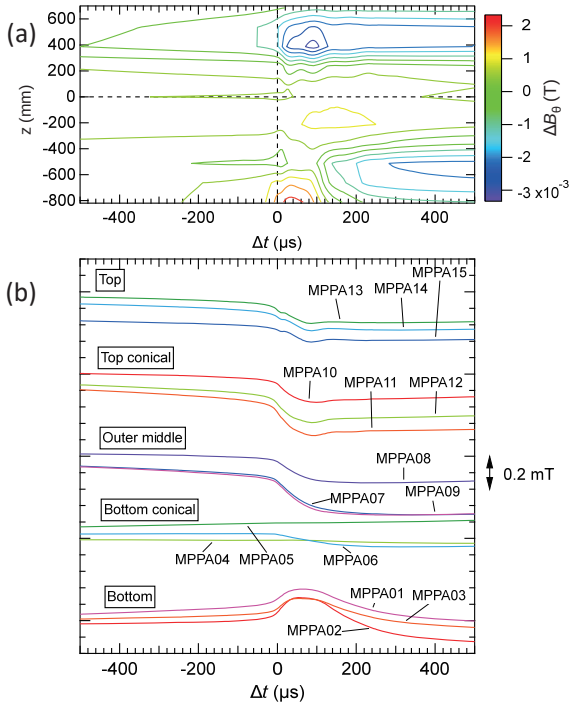

Fig. 4 Magnetic field variations during the event, which are observed by pick-up coils (a) at inner poloidal array and (b) at outer poloidal array. (a) is a contour plot and (b) is time traces with vertical offset.

electron density (n_{el}), emission intensity (H_α), and the raw signal of the representative pick-up coil at the inner equatorial plane (MPCSZ0) in Fig. 3 (a). Large spikes of a few tens of T/s in MPCSZ0 are observed to be synchronized with decays in I_p. Large events are accompanied by transient rises in n_{el}. Figure 3 (b) displays expanded view of the large event, which is ensemble-averaged over a few tens of events, with the peak time just before the drop in I_p as a condition. Here, the criterion for large events was that the width of change in the line-integrated density (Δn_{el}) exceeded 2×10^{16} m^{-2}. I_p waveform shows a slight increase, or a hump, just before the drop, followed by a decrease of 2 kA or more with a decay constant of a few milliseconds. The n_{el} initially decreases slightly but rises with the drop in I_p. H_α also exhibits an increase with the drop in I_p.

Figure 4 illustrates magnetic field fluctuations during large SCE–I events. All raw coil signals are integrated to display the range of displacement and ensemble-averaged using the same conditions as in Fig. 3 (b). During the event, the poloidal magnetic field strength decreases on the upper side and increases on the lower side. The direction of the magnetic field is positive in the direction created by the plasma current. Figure 4 suggests that the entire plasma rapidly moves downward vertically at a velocity of approximately 20 km/s. The observed decrease in the field strength from the equatorial plane to the bottom conical portion on the outer side indicates that the plasma simultaneously shifts inward as it moves downward. This series of movements has been captured and confirmed using a high-speed camera. The increase in H_α emission intensity may be attributed to the enhancement of recycling gas injection from the lower divertor or inner center stack (CS) plates, where the plasma collides, leading to an increase in density immediately following the event. The initial slight decrease in n_{el} should be partly attributed to the downward shift of the plasma while the horizontal sight of the microwave interferometer is on the equatorial plane, and partly attributed to the loss of plasma.

3.2 SCE–II: current rise events

Another type of repetitive sudden change event in plasma current has been observed. This event, referred to as SCE–II, is less periodic than SCE–I but highly repetitive when observed. A distinguishing characteristic of SCE–II is that the direction of the current change is positive, which is opposite to that of SCE–I.

The waveforms of SCE–II are depicted in Fig. 5, along with ensemble-averaged traces. H_α emission intensity exhibits clear spikes, concurrent with the magnetic field and corresponding rise in n_{el}. Although transient, this event involves an increase in current and merits attention. Based on the changes in the magnetic field profile at the inner poloidal array, it is suggested that the poloidal field strength rises in accordance with the rise in I_p while the vertical position of the plasma remains nearly unchanged. The area with the most significant change is slightly below the equatorial plane. Since the H_α increases, the interaction between the plasma and limiters should be enhanced somewhat during this event. The fast camera image suddenly showed intense luminescence in the entire plasma and no apparent displacement was observed.

3.3 SCE–III: largest events

Distinct from SCE–I and SCE–II, a rather rare event

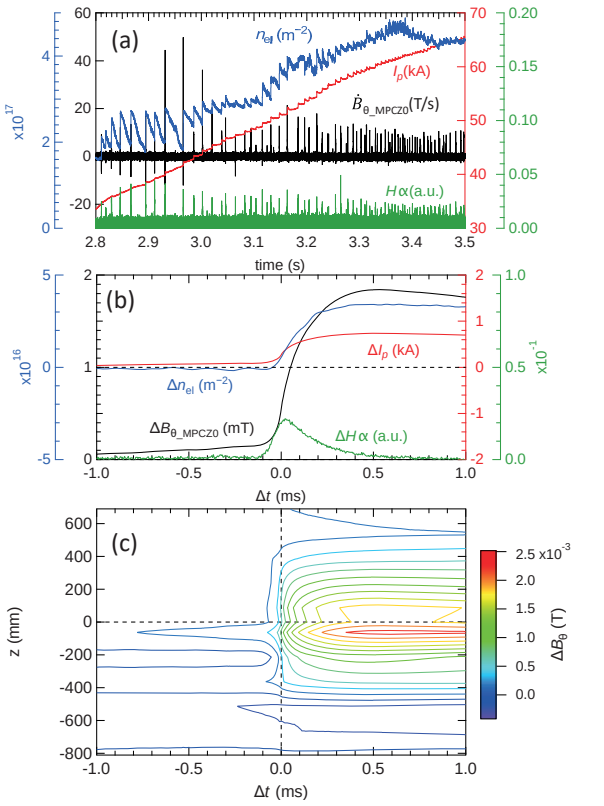

Fig. 5 (a) Discharge waveforms during repetitive SCE–II, (b) expanded traces with a conditional ensemble-average and (c) contour plot of the field displacement at the inner poloidal array.

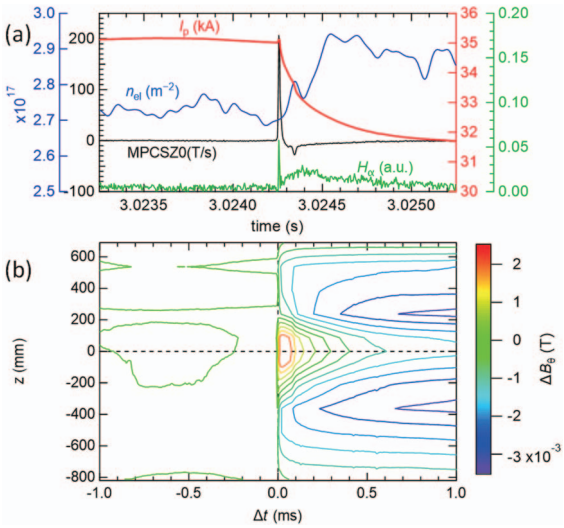

Fig. 6 (a) Typical waveforms and (b) contour plot of poloidal magnetic field variation at inner poloidal array during SCE–III.

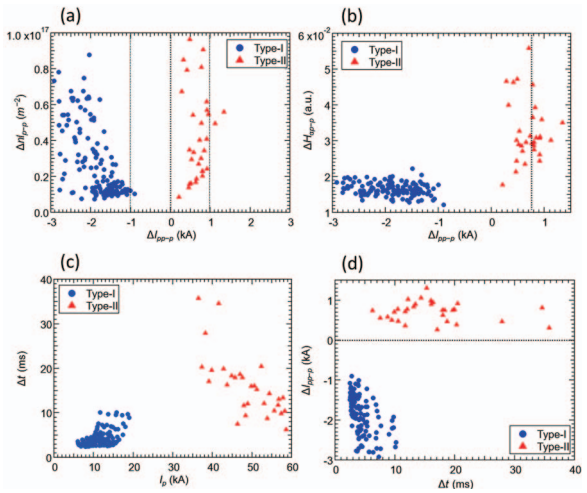

Fig. 7 Comparison of statistics between SCE–I and SCE–II. Change widths of (a) n_{el} and (b) H_α vs change width of plasma current ΔI_p and (c) event interval time Δt vs I_p, (d) I_p vs Δt.

referred to as SCE–III has been observed, with its typical waveforms and contour plot of the poloidal magnetic field displacement at the inner poloidal array shown in Fig. 6. Due to the wide variety of its scale, ensemble averaging is not performed; however, the relationship between the waveforms can be understood straightforwardly without being obscured by noise. The magnetic field decreases as the current decays, but it rises momentarily near the inner equator, exhibiting a faster timescale for field variation. In the event shown in Fig. 6, the amplitude of the spike in MPCSZ0 reaches 200 T/s, which is an order of magnitude higher than that of SCE–I and SCE–II. H_α shows sharp spike followed by gradual increase. The fast camera image suddenly showed intense luminescence in the entire plasma with leaving evidence of high-intensity X-ray radiation on the Charge Coupled Device (CCD).

4. Discussion

Figure 7 statistically compares the repetitive nature of SCE–I and SCE–II along with their effects on n_{el} and H_α. Firstly, it is evident from Figs. 7 (a) and 7 (b) that all events are accompanied by a positive increment in n_{el} and H_α. The horizontal axis in these figures represents the change in plasma current width (ΔI_p) as an indicator of the impact of an event on plasma configuration. A positive correlation exists between the change widths of line density (Δn_{el}) and $|\Delta I_p|$ for SCE–I. The larger the event impact ($|\Delta I_p|$), the more recycling gas appears to be injected. Compared to SCE–I, SCE–II tends to have higher Δn_{el} and ΔH_α with smaller $|\Delta I_p|$. This is partly because the sights of a microwave interferometer and a spectroscopy monitoring H_α are located around the equatorial plane, and the plasma center remains in position during SCE–II events but moves downward during SCE–I events.

In Figs. 7 (c) and 7 (d), the interval time between repetitive events (Δt) is plotted in relation to the event occurrence region, measured with I_p, and the event impact, measured with ΔI_p. SCE–I occurs in a relatively low I_p region of less than 20 kA. Positive correlations exist between Δt and I_p and between $|\Delta I_p|$ and Δt, indicating that the larger the events, the longer the wait time, and larger events tend to occur at higher I_p. This tendency resembles a phe-

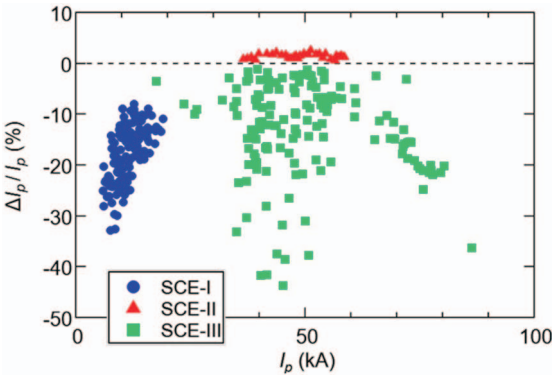

Fig. 8 Summary of sudden change events measured for non-inductive plasma current start-up on QUEST; those impact and region of occurrence.

nomenon with a certain threshold, such as the common sawtooth oscillation, in terms of storing energy, releasing it, and storing it again. Additionally, SCE–I was often observed in a specific series of discharges when the plasma shape was somewhat more vertically elongated than usual. Along with the experimental observation of rapid vertical displacement, the most likely physical mechanism appears to be vertical instability. However, there is an interesting aspect—the recovery from a grown-up event. This recovery is potentially due to the effect of energetic electrons dominating plasma current when enhanced by oblique injection of electron-cyclotron waves. In such cases, as energetic electrons are lost along with vertical plasma displacement, the current quickly decreases, and this decrease acts to stabilize the instability, possibly leading to recovery.

SCE–II has been observed in the middle I_p region of 35 - 60 kA so far. The range of Δt is wide and irrelevant to both I_p and ΔI_p, making it completely different from SCE–I. Although not shown in Fig. 7, the situation for SCE–III is somewhat like SCE–II in terms of its randomness. From the current measurements, SCE–II and SCE–III seem to occur randomly, without any discernible regularity.

SCE–III occurs once or at most several times in a single discharge. Not all discharges exhibit SCEs, but some do. Unlike SCE–I and SCE–II, the occurrence region of I_p is not yet limited for SCE–III, and its impact, measured by $\Delta I_p/I_p$, approaches almost 50%, meaning that half of the poloidal field produced via the current for confinement is lost during the event (see Fig. 8). Therefore, SCE–III is the most concerning event when considering further increases in plasma current with planned higher heating powers on QUEST.

So-called internal reconnection event (IRE) is known to occur in STs due to several instabilities [7–9]. When grown-up modes merge, magnetic reconnection occurs and the magnetic topology changes accordingly. If inner hot region is connected to outer cold region with a single field line due to the topology modification, internal hot plasma will be expelled toward outside along the pressure gradient. At that time, it is often observed that the current profile suddenly broadens, leading to a transient rise in the plasma current to compensate the sudden change in the plasma inductance. It is also observed that the corresponding toroidal electric field produces tails on velocity distribution of ions and electrons [10]. Thus, in a situation like QUEST where fast electrons dominate the plasma current, the transient response of fast electrons is speculated to play an important role. In SCE–II and SCE–III, radiation of intense hard X-rays is observed. Since the effects of IRE varies with detailed profiles of plasma parameters and magnetic field configuration, IRE may be related to SCE–II or both, including SCE–III. Many observations have been reported on STs so far. Therefore, we believe that IRE is the most probable trigger, and plan to detect the instabilities that cause IRE. Improvements in the magnetic measurements in the low-field side and internal thermal plasma measurements with high time resolution are required for this purpose.

5. Summary

In summary, to observe fast magnetic phenomena, magnetic pick-up coils with over 500 kHz frequency response were installed inside the vacuum vessel of QUEST. Two toroidal arrays and one poloidal array are useful in clarifying the global characteristics of phenomena accompanying magnetic perturbations. Using these coils, sudden change events in plasma current were measured and classified into three categories referred to as SCE–I, II, and III. SCE–I is a rapid vertical displacement event, SCE–II exhibits a transient current rise, and SCE–III is a large current drop event. SCE–III has a significant impact on plasma configuration and may lead to a disruption in future planned discharges with higher heating powers.

At present, no precursors have been found. Since the coils located in the outer region have low sensitivity to small-amplitude fluctuations due to the long distance and shielding material between the sensor and the plasma, these coils may miss precursor signals even if some instabilities that cannot be picked up by the inner coils occur. Coils that can withstand higher temperatures using ceramics will be developed and placed in front of hot walls. Additionally, high-speed internal measurements, such as electron cyclotron emission (ECE) and absolute extreme ultraviolet (AXUV), will be employed in future studies.

[1] K. Hanada *et al.*, Plasma Fusion Res. **5**, S1007 (2010).
[2] H. Idei *et al.*, Nucl. Fusion **57**, 126045 (2017).
[3] H. Idei *et al.*, Nucl. Fusion **60**, 016030 (2020).
[4] Y. Shi *et al.*, Nucl. Fusion **62**, 086047 (2022).
[5] T. Onchi *et al.*, Phys. Plasmas **28**, 022505 (2021).
[6] T.C. Hender *et al.*, Nucl. Fusion **47**, S128 (2007).
[7] A. Sykes, Plasma Phys. Control. Fusion **36**, B93 (1994).
[8] I. Semenov *et al.*, Phys. Plasmas **10**, 664 (2003).
[9] N. Mizuguchi, T. Hayashi and T. Sato, Phys. Plasmas **7**, 940 (2000).
[10] P. Helander *et al.*, Phys. Rev. Lett. **89**, 235002 (2002).